Broadly neutralizing human antibody that recognizes the receptor-binding pocket of influenza virus hemagglutinin

James R. R. Whittle[a], Ruijun Zhang[b], Surender Khurana[c], Lisa R. King[c], Jody Manischewitz[c], Hana Golding[c], Philip R. Dormitzer[d], Barton F. Haynes[b,e,f], Emmanuel B. Walter[b,g], M. Anthony Moody[b,g], Thomas B. Kepler[b,h], Hua-Xin Liao[b,e], and Stephen C. Harrison[a,1]

[a]Laboratory of Molecular Medicine, Children's Hospital, Harvard Medical School and Howard Hughes Medical Institute, Boston, MA 02115; [b]Duke Human Vaccine Institute and Departments of [e]Medicine, [f]Immunology, [g]Pediatrics, and [h]Biostatistics and Bioinformatics, Duke University Medical Center, Durham, NC 27710; [c]Division of Viral Products, Center for Biologics Evaluation and Research, Food and Drug Administration, Bethesda, MD 20892; and [d]Novartis Vaccines and Diagnostics, Cambridge, MA 02139

Contributed by Stephen C. Harrison, July 15, 2011 (sent for review June 23, 2011)

Seasonal antigenic drift of circulating influenza virus leads to a requirement for frequent changes in vaccine composition, because exposure or vaccination elicits human antibodies with limited cross-neutralization of drifted strains. We describe a human monoclonal antibody, CH65, obtained by isolating rearranged heavy- and light-chain genes from sorted single plasma cells, coming from a subject immunized with the 2007 trivalent influenza vaccine. The crystal structure of a complex of the hemagglutinin (HA) from H1N1 strain A/Solomon Islands/3/2006 with the Fab of CH65 shows that the tip of the CH65 heavy-chain complementarity determining region 3 (CDR3) inserts into the receptor binding pocket on HA1, mimicking in many respects the interaction of the physiological receptor, sialic acid. CH65 neutralizes infectivity of 30 out of 36 H1N1 strains tested. The resistant strains have a single-residue insertion near the rim of the sialic-acid pocket. We conclude that broad neutralization of influenza virus can be achieved by antibodies with contacts that mimic those of the receptor.

B-cell lineage | affinity maturation | X-ray crystallography

The well-known seasonal drift of influenza virus antigenicity accounts for the absence of long-term immune protection in previously infected individuals. The hemagglutinin (HA), a trimeric surface glycoprotein that binds the viral receptor and promotes fusion and penetration from low-pH endosomes, is the principal surface antigen on influenza virions (1). HA presents conserved and variable epitopes, but neutralizing antibodies against the latter dominate the response to immunization and infection (2).

The receptor for influenza virus is sialic acid, attached by terminal α-2,3 or α-2,6 linkage to glycans on glycoproteins or glycolipids (reviewed in ref. 3). Most neutralizing antibodies block cell attachment, either because their footprint overlaps the receptor-binding site or because they exert steric interference when bound elsewhere on the HA surface (2). Two mouse monoclonal neutralizing antibodies, for which structures of Fab:HA complexes have been determined, have loops that project into the sialic-acid binding pocket on HA and present an aspartic-acid side chain roughly where the sialic-acid carboxylate would be (4, 5), but both of these antibodies also have extensive contacts with other surface regions, in which escape mutations could occur more readily than in the receptor site.

We describe identification and characterization of a human monoclonal antibody with its principal contacts in the receptor pocket. This antibody, designated CH65, was found by isolating rearranged heavy- and light-chain genes from sorted single plasma cells, obtained from a subject who had received the 2007 trivalent vaccine. CH65 neutralizes a remarkably broad range of H1 seasonal isolates spanning more than three decades. Its 19-residue heavy-chain complementarity-determining region 3 (CDR-H3) inserts into the receptor pocket, mimicking many of the interactions made by sialic acid. Both heavy- and light-chain CDRs participate in more restricted, additional contacts with the outward-facing surface of HA1. The inferred, unmutated ancestor of CH65 differs from the affinity matured antibody at 12 positions in the heavy-chain variable domain, and at 6 in the light-chain variable domain. The human B-cell repertoire thus includes the potential to generate antibodies directed primarily at the receptor binding site. The large number of seasonal H1 viruses neutralized by antibody CH65 suggests that such responses are ordinarily too rare to select for resistance, or that resistance comes at too great a fitness cost—as would be the case if potential escape mutations were to compromise receptor binding.

Results

Clonal Lineage of a Broadly Neutralizing Antibody. Rearranged Ig V_H and V_L genes were isolated by RT/PCR from peripheral blood mononuclear cells, collected from a subject 1 wk after vaccination with the 2007 trivalent inactivated vaccine (TIV) (6). Among the clonal lineages detected by sequencing the rearranged genes was the three-member clone (mAbs CH65, CH66, and CH67) shown in Fig. 1*A* (6). The inferred sequence of the unmutated common ancestor (UCA) of the clonal lineage of antibodies CH65, CH66, and CH67 is unambiguous, except at position 99 of the heavy chain, which might be either glycine or alanine. Fig. 1*B* shows an alignment of the amino acid sequences of each antibody to the UCA. All three mature antibodies bind the H1 HA present in the vaccine (A/Solomon Islands/3/2006) with about equal affinity; the UCA binds much more weakly. We chose to focus our analysis on CH65. Its heavy chain differs from the UCA at 12 positions in the variable domain; its light chain, at 6.

Breadth of Neutralizing Activity. We expressed both CH65 IgG1 and its Fab in 293T cells by transient transfection and purified it as described in *Methods*. We tested neutralization against a large panel of H1 isolates from the past 30 y, including vaccine strains from 1977, 1991, and 1995, and observed strikingly broad potency (Table 1). The antibody neutralized H1N1 strains isolated as

Author contributions: J.R.R.W., R.Z., H.G., P.R.D., B.F.H., T.B.K., H.-X.L., and S.C.H. designed research; J.R.R.W., R.Z., L.R.K., J.M., M.A.M., T.B.K., and H.-X.L. performed research; E.B.W. contributed new reagents/analytic tools; J.R.R.W., R.Z., S.K., L.R.K., J.M., H.G., B.F.H., M.A.M., T.B.K., H.-X.L., and S.C.H. analyzed data; and J.R.R.W., H.G., P.R.D., B.F.H., and S.C.H. wrote the paper.

The authors declare no conflict of interest.

Freely available online through the PNAS open access option.

Data deposition: Coordinates have been deposited in the Protein Data Bank, with PDB ID 3SM5.

[1]To whom correspondence should be addressed. E-mail: harrison@crystal.harvard.edu.

This article contains supporting information online at www.pnas.org/lookup/suppl/doi:10.1073/pnas.1111497108/-/DCSupplemental.

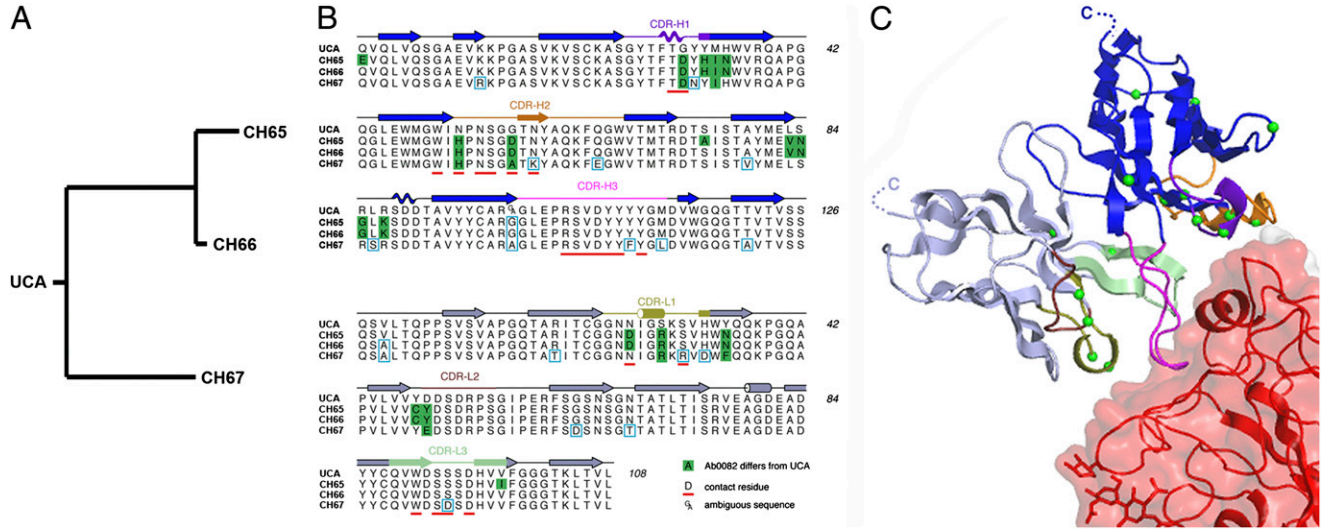

Fig. 1. (*A*) Inferred lineage of clone 860. (*Left*) The unmutated common ancestor (UCA) of the three antibodies (shown by their numbers, *Right*) isolated from the donor. (*B*) Alignment of heavy-chain (*Upper*) and light-chain (*Lower*) sequences in the lineage. Positions at which CH65 differs from the UCA are highlighted in green; those at which one of the other antibodies differs are boxed in blue; residues that contact HA in the complex are underscored in red. (*C*) Contact of the Fab from CH65 with HA1. Heavy chain in dark blue; light chain in light blue; CDRs in colors as labeled in *B*; and HA in red, with the atomic surface shown as a partly transparent overlay. Residues that have mutated from the UCA are marked at Cα positions by green spheres.

early as 1986, covering 21 y of antigenic drift. As expected, it neutralized A/Solomon Islands/3/2006, the H1 component of the 2007 vaccine. Of the 36 strains tested, it failed to neutralize only six, including the 2009 pandemic strain, A/Texas/36/1991, and A/USSR/90/1977. Too few HA-directed human monoclonal antibodies have been characterized for systematic comparison, but neutralization by serum samples does not ordinarily exhibit this degree of breadth.

Structure of CH65:HA. We crystallized a complex of the mAb CH65 Fab with the HA ectodomain from A/Solomon Islands/3/2006 (HA^{SI}), recorded diffraction to a minimum Bragg spacing of 3.2 Å (Table S1), and determined the structure by molecular replacement as outlined in *Methods*. The asymmetric unit of the crystal contains a single copy of the HA trimer, with three bound Fabs (Fig. 2). Our final model includes all HA1 and HA2 residues in the expressed protein, except four disordered residues at the C terminus of HA1. The electron density maps showed evidence for *N*-linked glycosylation at all eight potential sites on each monomer, and we could model one or more sugar residues at five of these positions. The Fab is well ordered, except residue 1 of the light chain and residues 141–147 of the heavy chain; these residues are all far from the binding site.

A/Solomon Islands/3/2006 (this work) and A/Puerto Rico/8/1934 (7) are, to our knowledge, the only seasonal H1N1 strains for which a structure of the HA has been determined; others are either pandemic strains or animal influenza strains. Comparison, using the program DALI, shows that HA^{SI} is similar to other H1N1 HAs, such as those of the pandemic isolates from 2009 [Cα RMSD 0.9 Å over 495 aligned residues, 79% sequence identity; PDB IDs 3LZG (8) and 3LYJ (9)] and 1918 [Cα RMSD 1.5 Å over 495 aligned residues, 85% sequence identity; PDB IDs 3LZF (8) and 1RUZ (7)] and the seasonal isolate from 1934 [Cα RMSD 1.5 Å over 482 aligned residues, 86% sequence identity; PDB ID 1RVZ (7)]. The vestigial esterase domain of HA^{SI} resembles that of the 2009 HA more closely than it does those from the 1918 and 1934 HAs.

MAb CH65 binds the globular head of the HA trimer (Figs. 1*C* and 2*A*). The epitope includes both the receptor site and the antigenic site designated Sb in an early analysis of H1 sequences (10) (Fig. 2*D*). The contact buries 858 $Å^2$ on the antibody and 748 $Å^2$ on HA1. All three CDRs of the heavy chain, as well as CDR-L1 and -L3 of the light chain, participate in the interface (Figs. 1*C* and 2 *B*–*D* and Fig. S1). CDR-H3 inserts into the receptor site. Seven of its 19 residues contribute 402 $Å^2$ of buried surface area, or 47% of the complete interface. The other CDRs form flanking interactions. CDR-L3 contacts the N-terminal end of the short α-helix, site Sb, at the edge of the receptor pocket, and CDR-H1 and -H2 contact a loop that protrudes from HA1 adjacent to the C terminus of that short α-helix. Analysis of the neutralized strains for which sequences are known shows little variation within the antibody footprint (Table S2).

CDR-H3 of mAb CH65 Compared with the Receptor. Because CDR-H3 inserts into the receptor site, we compared this structure to that of the human receptor analog LSTc (sialic-acid-α2,6-galactose-β1,4-*N*-acteylglucosamine) bound to 1934 HA (PDB ID 1RVZ: ref. 7) (Fig. 3). In CH65, Asp107 at the tip of CDR-H3 accepts hydrogen bonds from the backbone amide of HA1 Ala137 and the sidechain hydroxyl of Ser136; it also has a favorable charge interaction with the guanidinium of Arg226. (Arginine is found only rarely at position 226; glutamine is more common. Arg226 adopts a kinked conformation in the crystal structure; a glutamine would fit readily, with its Nε in the same position as the corresponding atom of the arginine side chain.) The backbone amide of Val106 in the antibody donates a hydrogen bond to the carboxyl oxygen of HA1 Val135, and the nonpolar sidechain of Val106 is in van der Waals contact with HA1 Trp153 and Leu194. In receptor analog LSTc, the carboxylate group of sialic acid has the same contacts with HA1 as does the (chemically analogous) sidechain of Asp107, and the amide and methyl of the acetamido group interact with HA in the same way as just described for the amide and side chain of Val106. A van der Waals contact between Leu194 and the 7-hydroxyl of the sialic-acid glycerol group, hydrogen bonded with the acetamido carbonyl, corresponds to a contact between Leu194 and Val106 Cα in the CH65 complex. In short, except for some interactions of the 8- and 9-positions of the glycerol, mAb CH65 mimics most of the chemical groups on the human receptor that interact with HA.

Glycosylation. Glycosylation at antigenic sites is an important mechanism of immune evasion by influenza virus (2, 3, 11). In

Table 1. Broad neutralization of seasonal influenza strains A/H1N1 by human MAb CH65

H1N1 virus strain	MAb CH65 minimum effective concentration (μg/mL)
A/Solomon Islands/3/2006*,†	0.024
A/Kawasaki/6/1986	0.098
A/Victoria/36/1988	0.781
A/Florida/2/1993	0.012
A/Beijing/262/1995*	0.098
A/Shengzhen/227/1995	0.012
A/Johnnesburg/82/1996	0.012
A/Johannesburg/159/1997	0.098
A/Shanghai/2/1997	0.195
A/Nanchang/16A/1997	6.25
A/Moscow/13/1998	0.012
A/Ostrava/801/1998	1.0
A/New Caledonia/22/1999*	0.391
A/England/192/2000	0.012
A/Bangkok/163/2000	0.195
A/Brazil/74200/2000	0.488
A/Fujian/156/2000	0.488
A/Chile/4795/2000	0.006
A/Chile/8885/2001	0.195
A/Auckland/65/2001	0.195
A/Singapore/14/2001	0.049
A/Christchurch/4/2001	0.098
A/Russia/2187/2002	0.195
A/New York/26/2002	3.125
A/Christchurch/1/2003	0.195
A/Brazil/1403/2003	3.125
A/Mexico/268/2003	0.781
A/Canada/59/2004	0.098
A/Hong Kong/2637/2004	0.195
A/Brisbane/59/2007*	0.391
A/USSR/90/1977*	100
A/Texas/36/1991*	Neg
A/Wellington/47/1992	Neg
A/Shanghai/8/1996	Neg
A/Neimenggu/52/2002	Neg
A/California/07/2009(swine)*	Neg

*Strains that were included in seasonal vaccines.
†H1 component of the vaccine received by the subject.

HA^{SI}, glycosylation leaves sites Sb and Cb exposed, partially obscures site Ca, and entirely masks antigenic site Sa. Site Sa is the epitope recognized by antibody 2D1, the prototype for Ig-mediated immunity to 2009 H1N1 in survivors of the 1918 epidemic (8). Of the sidechains in contact with 2D1, 7/16 differ between HA^{SI} and 1918 HA; in comparison, only 3/16 differ between 2009 pandemic HA and 1918 HA. Because the HA of A/Solomon Islands/3/2006 is glycosylated at site Sa, neither vaccination with TIV-2007 nor prior infection with an A/Solomon Islands/3/2006-like strain could have elicited a 2D1-like immune response.

Affinity Maturation. The amino acid sequence of CH65 is the result of affinity maturation from its UCA. Analysis of the structure in light of its clonal lineage (Fig. 1) shows that the central interactions of the antibodies with HA have remained unchanged by affinity maturation. The CDR-H3 has not mutated, nor has the contact of the light-chain CDR-L3 with the N-terminal end of the short α-helix, site Sb. (Ser93 of CDR-L3 is Asp in lineage member CH67, but the consequences of that change, if any, are not evident from model building.) Elsewhere on the interaction surface of the antibody, changes to two residues create additional hydrogen bonds between the antibody and HA^{SI} (Fig. S1). Light-chain residues Asp26 and Arg29 in CDR-L1 have mutated from their respective germline counterparts, Asn and Ser. Asp26 accepts a hydrogen bond from HA Lys222. Arg29 is positioned to donate two hydrogen bonds to HA Asp225. Other changes, including those at position 31 (Gly to Asp) and positions 33–35 (Tyr-Met-His to His-Ile-Asn) may exert subtle effects on the conformation of CDR-H3.

Structural Basis for Resistance to Neutralization. Comparison of the sequences of the 36 tested strains shows that those resistant to CH65 have an insertion of a basic residue, Lys or Arg-133A, between positions 133 and 134, adjacent to the receptor site (Fig. S2). None of the neutralized strains for which the HA sequence is available has this insertion. Superposition onto the HA in our structure of an H1 HA with the insertion (A/California/04/2009), suggests an unfavorable contact of the carbonyl of the inserted residue with Val106 (Fig. S2).

Discussion

CH65 comes from an adult subject in the United States, who received the 2007 TIV 1 wk before donating a plasma sample. We can assume that the subject had been exposed to H1N1 influenza strains in the past, so that the antibodies we obtained, by screening with a panel of recombinant hemagglutinins (rHAs), were from a secondary response. Indeed, the number of mutations (overall frequency about 5%) is too great to have occurred within just 1 wk of a primary exposure. In the setting of TIV, a large fraction of the circulating antibody secreting plasma cells 1 wk postvaccination are influenza specific (12). Unlike other methods (e.g., phage display) for high-throughput analysis of human B-cell responses, the procedure we used to isolate CH65 detects paired rearranged V_H and V_L regions and hence reconstructs the complete antigen combining site of the native antibody (6).

The CH65 antibody belongs to a relatively small clonal lineage of detected sequences, but there were presumably other members not represented among the expressed antibodies. Because the plasma cell from which it came probably derived from a vaccine-stimulated memory cell, most of the mutations that separate it from the UCA probably occurred during the earlier primary response. The breadth of infectivity neutralization by CH65 implies that it might have arisen during nearly any of the seasonal outbreaks of the two decades preceding 2007, as only a small number of mutations during the secondary response could have produced a very tightly binding antibody from one of somewhat lower affinity.

The antigen combining site of CH65 has no markedly atypical structural features. It has contributions from V_H 1~2, D_H 1~1, and J_H 6 and from Vκ3~21 and Jκ2 (Table S3). The 19-residue heavy-chain CDR3 is of roughly average length (13). Its sequence in the mature antibody is the same as in the UCA. The VDJ recombination that gave rise to the coding sequence of the UCA included 17 nontemplated nucleotides (Fig. S3), so that 6 of the 14 CDR3 residues are encoded by the random insertions produced by imprecise joining. These 6 residues include Val106 and Asp107, which together make the most critical contacts within the sialic-acid pocket. The predicted nontemplated nucleotide additions are somewhat fewer than average at the V-D junction and somewhat greater than average at the D-J junction (13).

The tip of the CH65 heavy-chain CDR3 is a strikingly faithful mimic of the sialic-acid surface that contacts HA. Early work on influenza virus antigenic variation led to discussion of an apparent conflict between escape from neutralization and conservation of an exposed receptor binding site. The HA structure resolved the issue, by showing that the sialic-acid binding site is smaller than the footprint of a typical antibody and hence that mutations in the periphery of the receptor pocket can interfere with neutralization without blocking receptor attachment (14, 15).

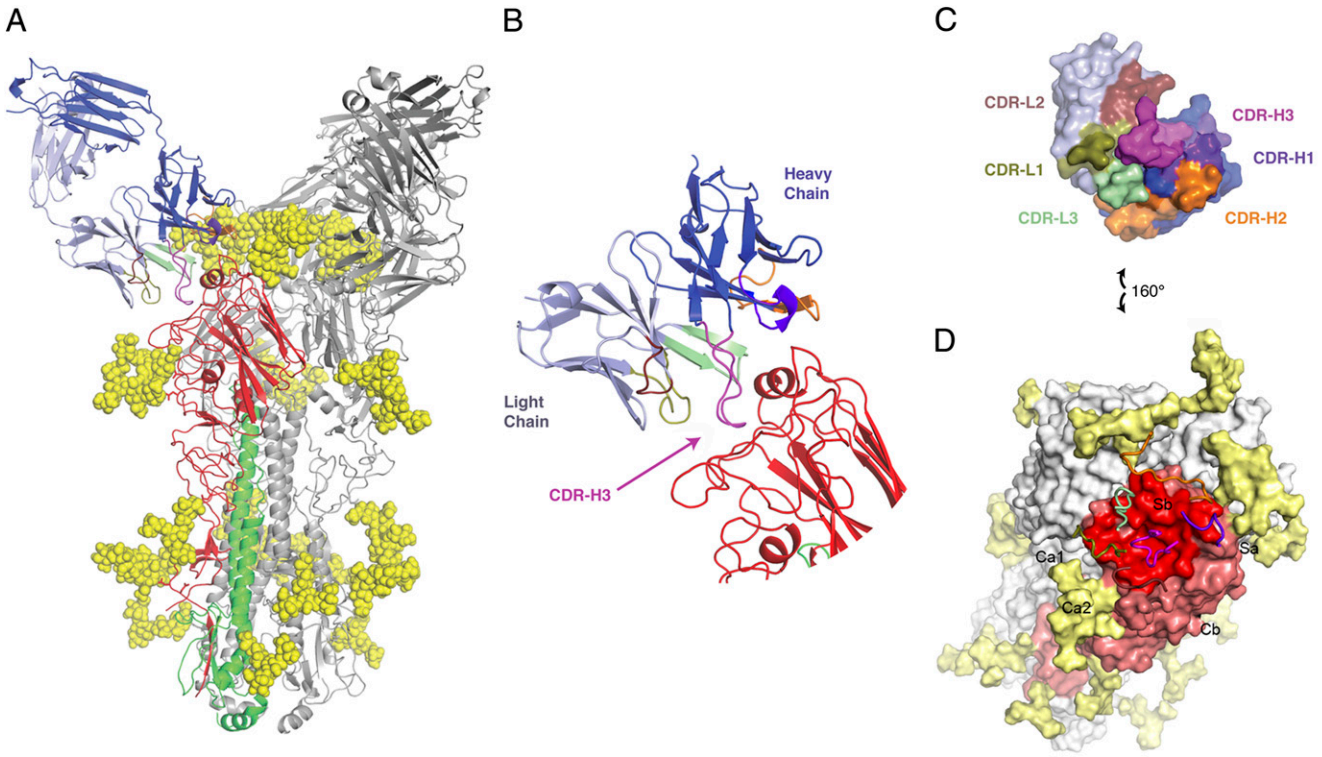

Fig. 2. (*A*) HA trimer with bound CH65 Fab. One HA chain is in red (HA1) and green (HA2); the other two chains are in gray; glycans are in yellow. The Fab bound to the colored HA chain is in dark blue (heavy chain) and light blue (light chain), with the contacting CDRs in colors as in Fig. 1. Glycans modeled with GlyProt server. (*B*) Blow-up of the variable region and its contact with HA1. Colors as in Fig. 1. Note that the heavy-chain CDR3 (magenta) projects into the receptor-binding pocket on HA1, whereas the remaining CDRs have more limited surface contacts. (*C* and *D*) Surface representation of the contact between Fab CH65 and HA1, opened up as shown by the arrows. The sialic-acid pocket on one HA subunit is in dark red; the rest of the subunit, in dull red; the remaining two subunits, in gray; and glycans, in yellow. (*D*) Worm representations of the CH65 CDRs are shown superimposed on the HA surface. The H1 epitopes (Sa, Sb, etc.) are labeled.

Indeed, variations affecting the susceptibility to neutralization by Ab CH65 map to sites that flank the receptor pocket but avoid any direct receptor contacts.

Two published structures of murine mAbs bound with H3 HAs show some degree of penetration into the receptor site—in both cases, by the heavy-chain CDR3. Neither mAb mimics the sialic-acid interaction as extensively as does CH65. In one [PDB ID 1KEN (5)], an aspartic acid side chain approaches the location of the sialic-acid carboxylate, but in an orientation that can accept a hydrogen bond only from the hydroxyl of Ser136 and not from the main-chain NH of Asn-137. In the other [2VIR (4)], a Tyr-Asp pair at the tip of the CDR3 has an orientation related to that of the Val-Asp pair in our CH65:HA complex, and the aspartic acid side chain has the same hydrogen-bonding pattern, but the mimicry does not extend to any of the interactions of the receptor acetamido group. H3 HAs have leucine, rather than glutamine or arginine at position 226, so that additional polar contact is not available.

Sites of mutations in naturally occurring, seasonal antigenic variants of HA are largely on the outward facing surface of HA1. Some relatively rare antibodies that bind a conserved site along the "stem" of the HA have come from phage-displayed libraries of unrelated, rearranged human V_H genes (all from V_H1–69). The structure and characteristics of CH65 show that it is also possible to elicit broadly neutralizing, receptor-binding site antibodies. We can draw a parallel with the broadly neutralizing, receptor-site antibodies against HIV-1 (e.g., antibody VRC01), which are reasonably close mimics of the functional receptor, CD4 (16).

An immunogen with an enhanced probability of eliciting a CH65-like response might protect against series of seasonal strains. A strategy for designing such an immunogen, on the basis of analysis of both the structure and the lineage, could include (in addition to the native HA) a component to induce a UCA-like primary response (17). Inspection of the differences between CH65 and its UCA suggests that the principal changes affecting affinity are in the light-chain CDR1, where mutations at positions 26 and 29 have introduced salt bridges with HA (Table S4). A modified HA, in which the same contacts instead gain stability from mutations in the antigen, might have the desired properties.

The lack of common resistance mutations among the many strains we tested suggests that Ab CH65 might be a useful template for a therapeutic antibody. Oseltamivir-resistant H1N1, which emerged rapidly beginning in 2007–2008, has become the predominant strain of seasonal influenza, and management of severe infection could benefit from a broadly reacting, immune-based therapeutic (18). Previous studies with a human mAb targeting the globular head of H5N1 predict that the effective neutralizing concentrations we find for CH65 would be protective in vivo (19).

Methods

Clinical Sample. MAbs CH65, CH66, and CH67 were obtained from a subject vaccinated with the 2007 TIV under a Duke Institutional Board approved human subjects protocol. The subject received the 2007–2008 Fluzone (Sanofi Pasteur), which contained A/Solomon Islands/3/2006(H1N1), A/Wisconsin/67/2005(H3N2), and B/Malaysia/2506/2004. Blood was drawn on day 7 post-vaccination, and peripheral blood mononuclear cells (PBMCs) were isolated and cryopreserved on the same day. Single plasmablasts were sorted into 96-well plates, using a panel of antibodies as described (6). Single-cell RT/PCR was carried out to obtain DNA for sequencing (6), which was done in both forward and reverse directions using a BigDye sequencing kit on an ABI 3700 (20) and assembled with a method based on quality scores at each position (21). Ig isotype was determined by local alignment with known sequences;

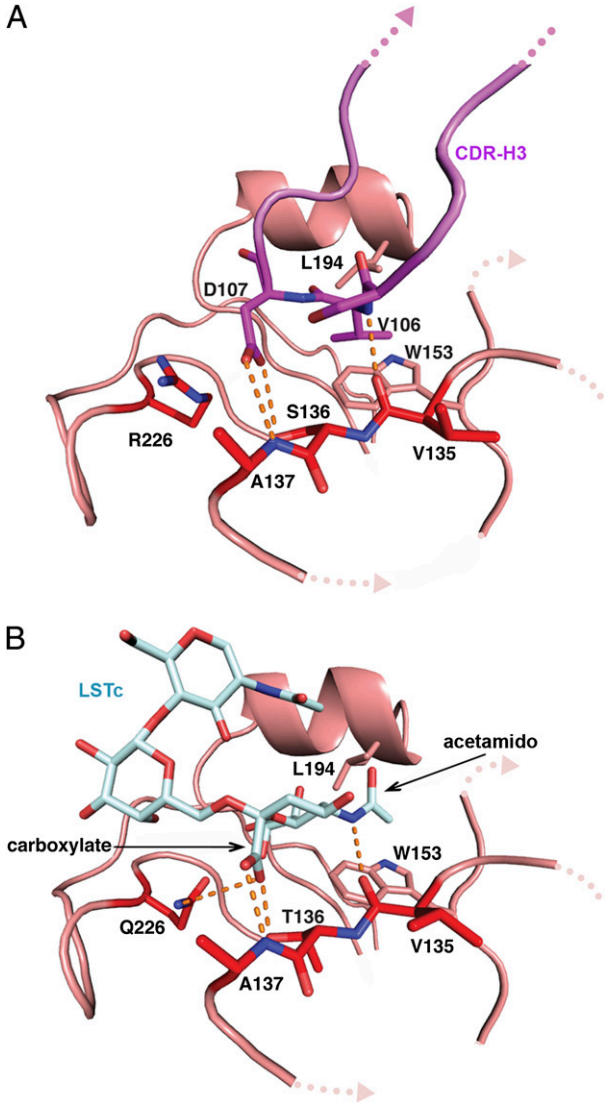

Fig. 3. Comparison of interactions from CH65 (*A*) and LSTc (*B*). Hydrogen bonds in the receptor site are shown as dashed lines.

V, D, and J region genes, CDR3 loop lengths, and mutation frequencies were determined by comparison with the inferred unmutated ancestor.

Lineage Analysis. The UCA was inferred using a Bayesian method by first determining the clonal tree by maximum likelihood using the program DNAML (22), and then computing the posterior joint distribution on gene segments and recombination sites, conditional on the inferred ML tree. The posterior probability mass function on nucleotides at each position was then obtained directly.

Expression and Purification of IgG and Fab. The variable regions of Ig heavy- and light-chain genes were isolated by RT/PCR from single plasma cells as described above (6). For production of purified full-length IgG antibody, the V_H and $V\kappa$ genes of CH65, CH66, and CH67 were cloned into a pcDNA 3.1 expression vector containing either the human IgG1 constant region gene or the κ-chain constant region gene (6). To produce the CH65 Fab, a 5′ primer, HV13274-F1 (5′-AAGCTTACCATGCCGATGGGCTCC-3′), was designed to contain a restriction site (HindIII) and sequences to anneal to the 5′ sequences of the Ig signal peptide, and a 3′ primer, HV13221H-R474 (5′-GAGCCCAAA-TCTTGTGACAAATGATCTAGA-3′) was designed to contain a restriction site (XbaI) and to introduce a stop codon after the sequence (5′-TCTTGTGACAAA-3′), encoding amino acid residues, SCDK, just before the hinge of the human IgG1 constant region. PCR amplification, using these primers and the full-length IgG1 heavy chain gene as template, yielded the Fab gene, which was cloned into pcDNA3.1/hygro (23). Recombinant, intact, CH65 IgG1 and its Fab were produced in 293T cells by cotransfection with the genes encoding heavy and light chains. The intact antibody was purified using antihuman IgG beads (Sigma); the Fab, using anti-L chain beads (Sigma) followed by FPLC gel filtration (6, 23).

Infectivity Neutralization. Infectivity neutralization was analyzed in a microneutralization assay based on the methods of the influenza reference laboratories at the Centers for Disease Control and Prevention (24). H1N1 historical virus stocks were provided by Vladimir Lugovtsev (Division of Viral Products, Center for Biologics Evaluation and Research, Federal Drug Administration, Bethesda, MD). All viruses were titrated on Madin Darby canine kidney (MDCK) cells and used at 100 times the 50% tissue culture infective dose (TCID50) per well (in triplicate). Twofold serial dilutions of mAb CH65, starting at 100 μg/mL, were mixed with virus stocks before addition to MDCK cell monolayers. The effective concentrations of antibody needed to inhibit at least 99% of viral infectivity are reported in Table 1.

HA Expression and Purification. Codon-optimized cDNA of the ectodomain of HA A/Solomon Islands/3/2006 was synthesized by GeneArt and subcloned into a pFastBac vector modified for ligation-independent cloning (LIC). The synthetic gene encoded a secretion signal at the N terminus, and, in place of the transmembrane domain, a thrombin cleavage site, a T4-fibritin "foldon" to promote proper trimerization, and a His6 tag at the C terminus. Trichoplusia ni (Hi-5) cells were infected with recombinant baculovirus. The supernatant was harvested at 48 h postinfection by centrifugation, concentrated and diafiltered against PBS with 40 mM imidazole, and loaded onto Ni-NTA resin. The protein was eluted, dialyzed, and incubated overnight with L-1-tosylamido-2-phenylethyl chloromethyl ketone (TPCK)-treated trypsin at 1:500 mass ratio to remove the trimerization and His6 tags and to cleave the HA0 precursor peptide. The protein was further purified by gel filtration chromatography on Superdex 200 (GE Healthcare).

Crystallization. The CH65 Fab and the A/Solomon Islands/3/2006 HA were incubated in 4.5:1 molar ratio, and the resulting 3:1 complex was separated from excess Fab by gel filtration chromatography on Superdex 200 in 10 mM Hepes pH 7.5, 150 mM NaCl. The complex was concentrated to an absorbance of 10 at 280 nm (~6 mg/mL). Crystals were grown in hanging drops over a reservoir containing 2.2 M ammonium sulfate, 100 mM Tris pH 7.5, and 5% PEG-400 at 18 °C. Crystallization was improved by microseeding. After 3–14 d, crystals were cryoprotected by adding reservoir solution supplemented with 15% glycerol to the drop, then harvested and flash cooled in liquid nitrogen.

Structure Determination and Refinement. Diffraction experiments were performed at beamline 24-ID-E at the Advanced Photon Source. A dataset at 3.2-Å resolution was collected from a single ~50 × 50 × 300 μm rod and processed using HKL2000 (Table S1). Molecular replacement (MR) calculations were performed with PHASER (25), using 1934 H1 HA [PDB ID 1RVZ (7)] as the starting model. Initial phases from MR enabled a search for Fab molecules by phased molecular replacement in MOLREP, using a library of Fab structures. The model was refined in CNS (26) by simulated annealing using deformable elastic network restraints and rebuilt in COOT (27). *N*-linked glycans from a high-resolution structure were fitted into experimental electron density maps where appropriate. Strong threefold noncrystallographic symmetry restraints were applied to HA and to each domain of the Fab throughout refinement, allowing variation in the angle between the conserved domain and the variable domain of the Fab. Finally, three cycles of individual positional and B-factor refinement in PHENIX (28) resulted in a model in good agreement with observed intensities (*R*/*R*free = 21.1/24.8%) (Table S1). Coordinates and diffraction data have been submitted to the PDB, accession number 3SM5.

ACKNOWLEDGMENTS. We thank Andrew Foulger, Robert Parks, Robert Meyerhoff, and Krissey Lloyd for antibody expression and binding assays; Ethan Settembre, Andrea Carfi, Yingxia Wen, and Kyoko Uehara for advice and assistance; and Vladimir Lugovtsev for maintaining the archived influenza type A strains used in the current study. This work is based upon research conducted at the Advanced Photon Source on the Northeastern Collaborative Access Team beamlines, which are supported by Award RR-15301 from the National Center for Research Resources at the National Institutes of Health (NIH). Use of the Advanced Photon Source, an Office of Science User Facility operated for the Department of Energy (DOE) Office of Science by Argonne National Laboratory, was supported by the DOE under Contract no. DE-AC02-06CH11357. The work was supported in part by the Division of AIDS, National Institute of Allergy and Infectious Diseases (NIAID), NIH with the Center for HIV/AIDS Vaccine Immunology NIAID Grant U19 AI067854. S.C.H. is an Investigator in the Howard Hughes Medical Institute.

1. Skehel JJ, Wiley DC (2000) Receptor binding and membrane fusion in virus entry: The influenza hemagglutinin. *Annu Rev Biochem* 69:531–569.
2. Knossow M, Skehel JJ (2006) Variation and infectivity neutralization in influenza. *Immunology* 119:1–7.
3. Wiley DC, Skehel JJ (1987) The structure and function of the hemagglutinin membrane glycoprotein of influenza virus. *Annu Rev Biochem* 56:365–394.
4. Fleury D, Wharton SA, Skehel JJ, Knossow M, Bizebard T (1998) Antigen distortion allows influenza virus to escape neutralization. *Nat Struct Biol* 5:119–123.
5. Barbey-Martin C, et al. (2002) An antibody that prevents the hemagglutinin low pH fusogenic transition. *Virology* 294:70–74.
6. Liao HX, et al. (2009) High-throughput isolation of immunoglobulin genes from single human B cells and expression as monoclonal antibodies. *J Virol Methods* 158:171–179.
7. Gamblin SJ, et al. (2004) The structure and receptor binding properties of the 1918 influenza hemagglutinin. *Science* 303:1838–1842.
8. Xu R, et al. (2010) Structural basis of preexisting immunity to the 2009 H1N1 pandemic influenza virus. *Science* 328:357–360.
9. Zhang W, et al. (2010) Crystal structure of the swine-origin A (H1N1)-2009 influenza A virus hemagglutinin (HA) reveals similar antigenicity to that of the 1918 pandemic virus. *Protein Cell* 1:459–467.
10. Caton AJ, Brownlee GG, Yewdell JW, Gerhard W (1982) The antigenic structure of the influenza virus A/PR/8/34 hemagglutinin (H1 subtype). *Cell* 31:417–427.
11. Wei CJ, et al. (2010) Cross-neutralization of 1918 and 2009 influenza viruses: Role of glycans in viral evolution and vaccine design. *Sci Transl Med* 2(24): 24ra21.
12. Wrammert J, et al. (2008) Rapid cloning of high-affinity human monoclonal antibodies against influenza virus. *Nature* 453:667–671.
13. Volpe JM, Kepler TB (2008) Large-scale analysis of human heavy chain V(D)J recombination patterns. *Immunome Res* 4:3.
14. Wiley DC, Wilson IA, Skehel JJ (1981) Structural identification of the antibody-binding sites of Hong Kong influenza haemagglutinin and their involvement in antigenic variation. *Nature* 289:373–378.
15. Wilson IA, Skehel JJ, Wiley DC (1981) Structure of the haemagglutinin membrane glycoprotein of influenza virus at 3 A resolution. *Nature* 289:366–373.
16. Zhou T, et al. (2010) Structural basis for broad and potent neutralization of HIV-1 by antibody VRC01. *Science* 329:811–817.
17. Ma B-J, et al. (2011) Envelope deglycosylation enhances antigenicity of HIV-1 gp41 neutralizing epitopes for broad neutralizing antibodies and their putative germlines. *PLoS Pathog*, in press.
18. Dharan NJ, et al.; Oseltamivir-Resistance Working Group (2009) Infections with oseltamivir-resistant influenza A(H1N1) virus in the United States. *JAMA* 301: 1034–1041.
19. Simmons CP, et al. (2007) Prophylactic and therapeutic efficacy of human monoclonal antibodies against H5N1 influenza. *PLoS Med* 4:e178.
20. Ewing B, Hillier L, Wendl MC, Green P (1998) Base-calling of automated sequencer traces using phred. I. Accuracy assessment. *Genome Res* 8:175–185.
21. Kepler TB, et al. (2010) Chiropteran types I and II interferon genes inferred from genome sequencing traces by a statistical gene-family assembler. *BMC Genomics* 11:444.
22. Felsenstein J (1981) Evolutionary trees from DNA sequences: A maximum likelihood approach. *J Mol Evol* 17:368–376.
23. Nicely NI, et al. (2010) Crystal structure of a non-neutralizing antibody to the HIV-1 gp41 membrane-proximal external region. *Nat Struct Mol Biol* 17:1492–1494.
24. Hancock K, et al. (2009) Cross-reactive antibody responses to the 2009 pandemic H1N1 influenza virus. *N Engl J Med* 361:1945–1952.
25. McCoy AJ, et al. (2007) Phaser crystallographic software. *J Appl Cryst* 40:658–674.
26. Brunger AT (2007) Version 1.2 of the Crystallography and NMR system. *Nat Protoc* 2: 2728–2733.
27. Emsley P, Cowtan K (2004) Coot: Model-building tools for molecular graphics. *Acta Crystallogr D Biol Crystallogr* 60(Pt 12 Pt 1):2126–2132.
28. Adams PD, et al. (2002) PHENIX: Building new software for automated crystallographic structure determination. *Acta Crystallogr D Biol Crystallogr* 58:1948–1954.